

Augmentation of the Performance of a Photovoltaic Cell: A Field Study

M.E. Zoreia*, M.R. Salem, R.K. Ali and K.M. Elshazly

Benha University, Faculty of Engineering at Shoubra, Mechanical Engineering Department,
108 Shoubra Street, Cairo 11689, Egypt

(*) Corresponding author (M.E. Zoreia): Tel: +201201116842

Email: me011573137097@gmail.com

Abstract

This work introduces a field study for the performance of a photovoltaic (PV) module under cooling with pure water or γ -Al₂O₃/water nanofluid with different nanoparticles volume concentrations ($0 \leq \phi \leq 1\%$) flows in straight or helical aluminium channels beneath the PV cell. The results showed that employing the helical channels configuration supplies the highest exergy efficiency along with the uppermost rise in the PV-electrical power. The average increases in the electrical output power are 21.8% and 27.9% when using the straight and helical channels, respectively. Additionally, increasing the nanoparticles fraction in the studied range and the cooling medium flow rate can augment the exergy efficiency. Compared with the standalone cell, the exergy efficiency increases at flow rate of 1 L/min by 76.4% at $\phi = 1\%$ with increasing the nanoparticles concentration from 0 to 1% for using the helical channels.

Keywords: Photovoltaic, Nanofluid, Exergy efficiency, Net power.

1. Introduction

The increased usage of fossil fuels in most fields of life have extremely dangerous influences on the environment. Furthermore, these sources of energy are not sustainable; it is predicted that the depletion of these sources' assets in the following 50 years. To overcome these issues, it was thought in sustainable energy sources, which are considered as new sources of clean energy. A key of the important sources among the sustainable energies is the solar energy [1]. Fortunately, Egypt is an investor's vision when it comes to solar energy as a sustainable energy resource; it owns an abundance of land and sunny weather.

Photovoltaic modules involve the innovation to change over sunlight directly into electrical energy. Nerveless, the characteristics of the PV module rely on many constraints including the panel temperature. The fraction of the absorbed solar radiation that is not changed over into electricity is converted into a thermal energy. Thus, numerous investigators devoted their considerations in decreasing the cells temperature to boost the electrical benefits [2]. A photovoltaic/thermal (PVT) hybrid solar system is a grouping of PV cell and solar thermal mechanism, which yield both electrical and heat energies from one combined module. The

basis behind the hybrid concept is that a panel converts the solar radiation to electrical energy with ultimate efficiency in the range of 5–20%, depending on the cell type. Over 80% of the incident radiation on the panels is not transformed to electricity, however either reflected or changed over to heat energy [3].

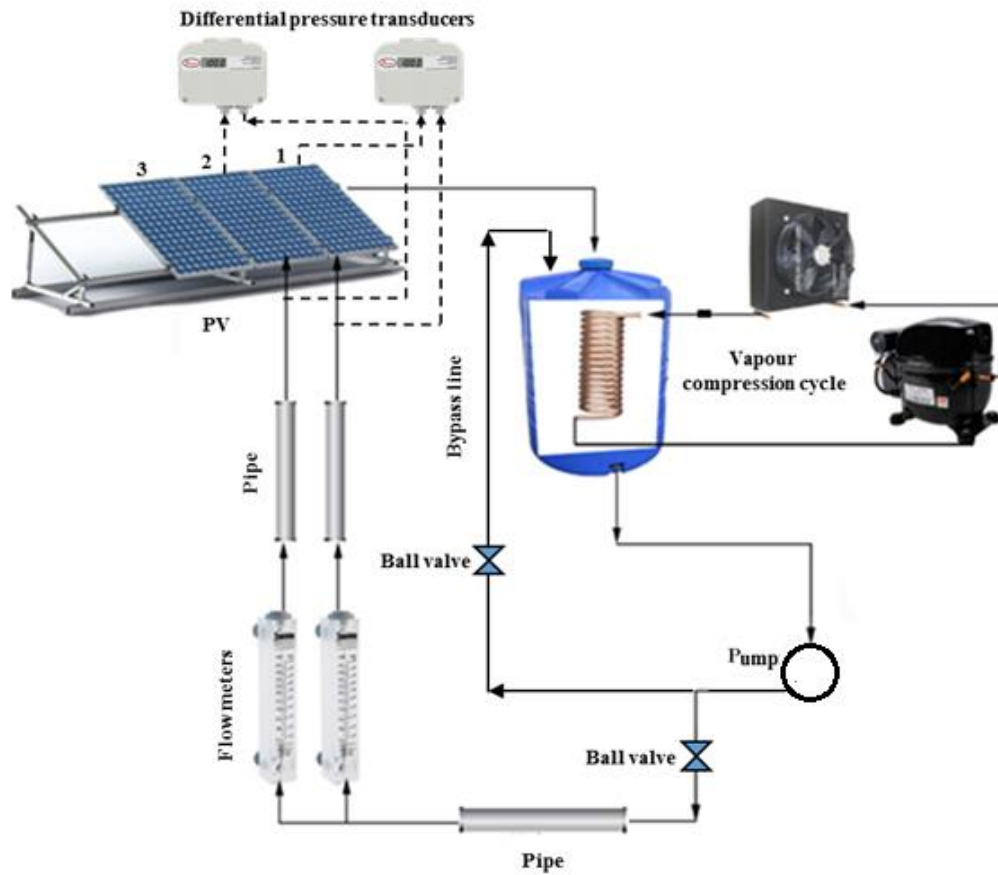
Cooling strategies for heat applications were introduced for PV cells to increase their electrical output power. In general, the cooling process requires a different system which will dispossess the thermal energy. The structure and repairs of that system can be costly and there is a potential that the cost of system repairing could exceed the advantages of the enhanced electrical output. Akbarzadeh and Wadowski [4] experimentally examined the influence of conducting a heat pipe to the rear surface of a PV cell. Anderson et al. [5] also reported the cooling of a PV panel using water heat pipe and aluminium fins. It was demonstrated that this cooling system is able to passively cool the PV cell. Huang et al. [6–8] experimentally tested the cooling of PV panel using a paraffin wax as a phase change material (PCM) in a rectangular aluminium basin attached to the rear surface of the panel. The results reported a reduction in the PV temperature by more than 3°C. Tonui and Tripanagnostopoulos [9] simulated the cooling attributes of a PV panel by a natural air flow in addition to attaching fins to the back surface. Jay et al. [10] investigated the output of PV/PCM system. The results showed an increment of 15–23% in the electrical efficiency. Cuce et al. [11] experimentally evaluated the effects of using a heat sink made of aluminium on the attributes of PV cells. The outputs showed an enhancement in the electrical power by about 20%. Teo et al. [12] inspected the enhancement of a PV output by passing air in parallel channels on the back surface of the cell. It was shown that the electrical efficiency was enhanced by 14%. Elmir et al. [13] numerically studied the cooling of a cell by applying Al_2O_3 /water nanofluid through a cavity behind the cell. The simulations indicated that using the nanofluids enhanced the rate of cooling with increasing the nanoparticles concentration. Ozgoren et al. [14] reported an enhancement in the conversion efficiency from 8% to 13.6% by flowing water under the solar panel. Ceylan et al. [15] experimentally assessed the effect of using a simple copper pipe behind the PV module. It was observed that the module conversion efficiency was augmented by 30%. Karami and Rahimi [16] experimentally assessed the heat exchange attributes in a PV module via Boehmite nanofluid as a coolant in conduits behind the cell. Accordingly, the electrical efficiency was increased by 21% and 38% for the straight and helical channels, respectively. Aldihani et al. [17] estimated the PV-electrical efficiency in Kuwait weather. The assessments showed that the dust fell the output power by 16%. Hasan et al. [18] reported a growth in the conversion efficiency by more than 10% due to applying PCM cooling. Nizetic et al. [19] recorded an enhancement of 16.3% in

the electrical conversion via employing water spray cooling. Salem et al. [20] tested the performance of a panel under cooling via pure water through straight or helical channels. It was reported that a maximum increment in the electrical efficiency by 38.4% was demonstrated when compared with the standalone panel. Tan et al. [21] assessed the performance of a solar panel under using PCM-fins cooling, which reduced the panel temperature by 15°C. Hasan et al. [22] reported the influence of employing a PCM on the module attributes. The authors indicated a growth of 5.9% in the conversion efficiency. Salem et al. [23] investigated the attributes of a cell cooling effect by engaging water and/or Al_2O_3 /PCM combination in straight conduits underneath the module. The authors concluded that the PV-cooling using 100% water supplied the highest electrical output power. The present work considers a hybrid PVT attributes in Cairo, which is one of the furthestmost energy-consuming places where a talented solar irradiation is available. The experiments aim to assess the helpfulness of the usage of $\gamma\text{-Al}_2\text{O}_3$ /water nanofluid in aluminium channels with straight and helical configurations in the PV cooling and using the thermal energy.

2. Experimental Setup

The experimental apparatus comprises three identical poly-crystalline 50 W PV panels, cooling facility, adjusted stand, and the gauging tools. The cold pure water or $\gamma\text{-Al}_2\text{O}_3$ /water nanofluid (directed to the conduits below the PV) loop comprises DC pump, flow meter, cooling unit with a thermostat, and the connecting pipes. Figure 1 (a and b) introduces a photograph and a layout for the experimental apparatus.





b) **Fig. 1: The experimental apparatus; (a) Photograph, (b) Layout.**

The modules characteristics are revealed in Table 1. The panels are being south oriented and fixed at the same tilt angle of 30° with the horizontal surface.

Table 1: Solar panels specifications.

Cell type	Poly-crystalline
Peak power ($Q_{a, max}$)	50 W
Dimensions	670*550*35 (± 1 mm)
Maximum power voltage (V_{mp})	18 V
Maximum power current (I_{mp})	2.78 A
Short circuit current (I_{sc})	3.06 A
Open circuit voltage (V_{oc})	21 V
Maximum system voltage	1000 V
Ordinary operating PV temperature	45°C

Two pallets of $640 \times 521 \times 18$ mm³ are fabricated from aluminium; one of them with helical channels, while the other is with straight channels (Fig. 2) and used for passing the cooling nanofluid. The aluminium material is selected because of its reasonable cost compared with its thermal conductivity (about 205 W/m.°C). The depth and width of channels used in both configurations are 10×10 mm² (aspect ratio of 1), while the spacing between the grooves is 10 mm.



Fig. 2: Helical and straight channels.

Gamma-alumina ($\gamma\text{-Al}_2\text{O}_3$) nanoparticles of 40 nm average size are used in the experiments. Their thermophysical properties are revealed in [Table 2](#).

Table 2: Properties of $\gamma\text{-Al}_2\text{O}_3$ nanoparticles.

Thermal conductivity (W/m. °C)	Density (kg/m ³)	Specific heat (J/kg. °C)
36	3600	773

The $\gamma\text{-Al}_2\text{O}_3$ /water nanofluid is prepared with five different nanoparticles volume loadings from 0 to 1%. Agitator (3450 rpm) is operated for 12 hours to get the stable and uniform suspension. The cooling unit is made of 20 litres tank; the cooling process to the desired temperature was achieved via a cooling unit of 1.5 kW capacity, based on a thermostat. There are three ports in the cooling tank; one of them is in the top covers of the tank, represents the inlet port from the channels. The other two ports are in the bottom, which represent the exit ports to the drain and to the DC-pump. A 4.2 W DC pump is linked to the tank to supply the conduits with the designed flow rate. Three variable resistances of $30\ \Omega \pm 1\%$ are used to fluctuate the load in the three panels' circuits.

A digital solar power meter is utilized to measure the incident solar radiation intensity, and a digital environmental meter is utilized for measuring the weather condition. Seven multimeters are employed in the circuit, to measure the current and voltage of the three modules along with the DC pump. To measure the temperatures in the overall setup, twenty-six K-type thermocouples are utilized. Twenty-four thermocouples are attached at both sides of the three cells, while two thermocouples are utilized to assess the inlet/outlet temperatures of the cooling nanofluid. The thermocouples are connected to a data acquisition system to record the

temperatures. Two identical flow meters; 0.002–2 L/min range, are incorporated to adjust the flow rate of the cooling nanofluid through the two channels configurations. According to the manufacturer’s data sheet, the meters are with accuracy of $\pm 2.5\%$ of full scale. Two identical digital pressure/differential pressure transducers are employed for measuring the pressure difference across the channels. The transducers are with a pressure drop range of 0–103.4 kPa, and of accuracy of $\pm 1\%$ of full scale.

3. Experimental Procedures and Data Reduction

The first step to record the data from the system is to fill the cooling tank with water from the domestic supply or with $\gamma\text{-Al}_2\text{O}_3$ /water nanofluid, the cooler and the pump are operated. By the thermostat, the temperature of the water ingoing the conduits ($25 \pm 0.5^\circ\text{C}$) is adjusted. In each run, the cooling fluid from the tank is circulated in the main line to the channels beneath the module as revealed in Table 3.

Table 3: Range of average operating conditions.

Parameters	Range or value
Cooling water/nanofluid flow rate, L/min	0–1
Cooling water/nanofluid inlet temperature, $^\circ\text{C}$	25
Volume concentration of the Al_2O_3 nanoparticles in water (ϕ), %	0–1

The PV surfaces are cleaned by a dry cloth from any accumulation of dust through the previous day. The three-electric circuits necessary for gauging the modules attributes, are assembled as illustrated in Fig. 3.

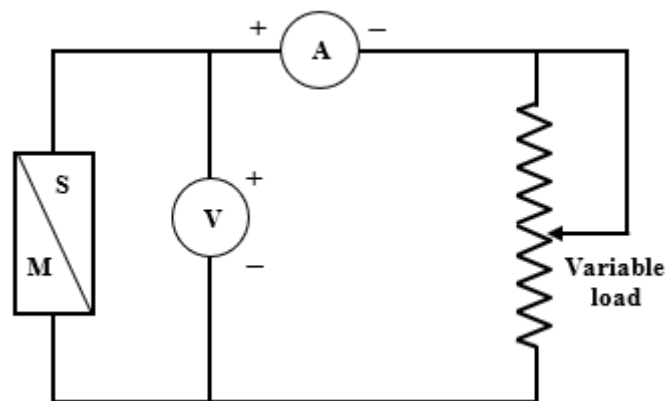


Fig. 3: Measurement circuit for the PV attributes.

After ensuring the entire circuit is running normally, the output wires are disconnected from the cells and connected each one to the variable load circuit one after one in a period that does not surpass 2 minutes. Then, the I-V curve is determined, and the optimum point is found as

revealed in Fig. 4. These actions are begun daily at 7 AM, before recording the first reading at 8 AM. The measurements are repeated every 30 minutes till sunset.

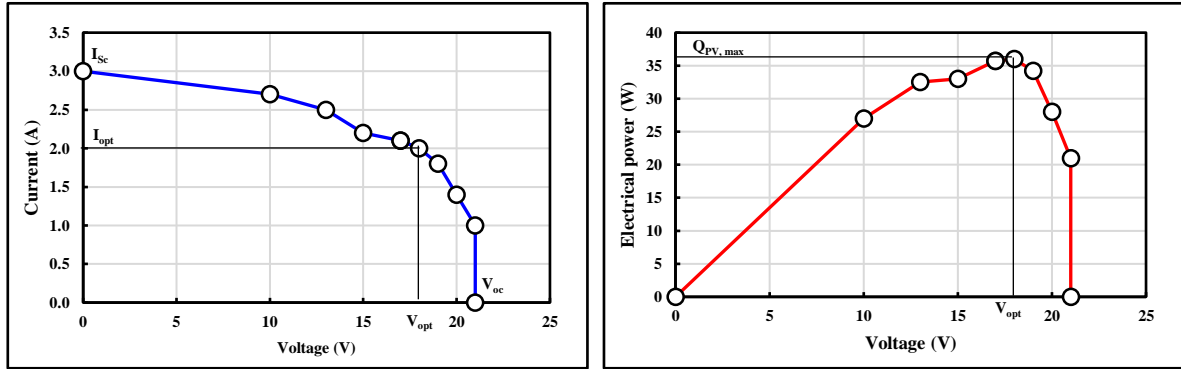


Fig. 4: Characteristic curves for the PV cell.

The following relations are utilized to analyse the PV characteristics.

$$Q_{in} = G_S \times A_{PV} \quad (1)$$

$$Q_{PV} = V \times I \quad (2)$$

$$Q_{PV_{max}} = V_{opt} \times I_{opt} \quad (3)$$

$$\eta_e = \frac{Q_{PV_{max}}}{Q_{in}} \quad (4)$$

$$Q_{th} = \dot{m}_{nf} C_{p,nf} (T_{nf,o} - T_{nf,i}) \quad (5)$$

$$\eta_{th} = \frac{Q_{th}}{Q_{in}} \quad (6)$$

$$\Delta T_{PV} = T_{PV_{ref}} - T_{PV_c} \quad (7)$$

$$T_{PV} = \frac{T_{PV_f} + T_{PV_b}}{2} \quad (8)$$

$$T_{PV_f} = \frac{\sum T_{PV,sf}}{4} \quad (9)$$

$$T_{PV_b} = \frac{\sum T_{PV,sb}}{4} \quad (10)$$

$$\Delta Q_e (\%) = \left[\frac{Q_c - Q_{ref} - W_p}{Q_{ref}} \right] \times 100 \quad (11)$$

$$W_p = V_p \times I_p \quad (12)$$

$$\eta_{EX,o} = \eta_e + \eta_{th} \left[1 - \frac{T_a}{T_{nf,o}} \right] \quad (13)$$

Equation (13) is used before in [20, 23]. For the properties of γ -Al₂O₃/water nanofluid, the density is as follows;

$$\rho_{nf} = \phi \rho_{np} + (1 - \phi) \rho_{bf} \quad (14)$$

In addition, for the specific heat, the proposed model by Xuan and Roetzel [24], Eq. (15), is applied;

$$C_{p_{nf}} = \frac{\varphi (\rho_{np} C_{p_{np}}) + (1 - \varphi)(\rho_{bf} C_{p_{bf}})}{\rho_{nf}} \quad (15)$$

4. Results and Discussions

to observe their similarity, the three cells conversion efficiencies are compared for non-cooling case under the same conditions (Fig. 5).

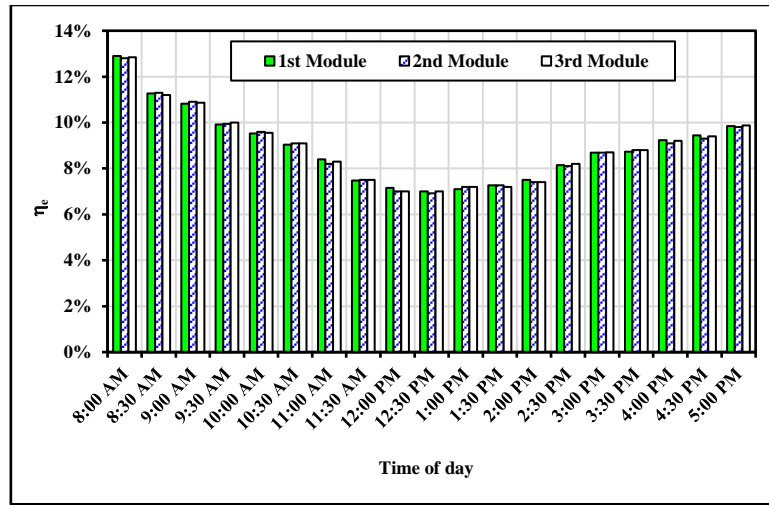


Fig. 5: Comparison between the three panels under the same conditions.

It is seen that there are tiny deviations between the efficiencies of the three panels, which confirm that they can be compared at different conditions.

4.1 Effect of The Channels Configuration

Figure 6 presents the recorded PV characteristics at different times of the day for the three tested panels; standalone panel and two cooled panels using straight and helical channels beneath the cells.

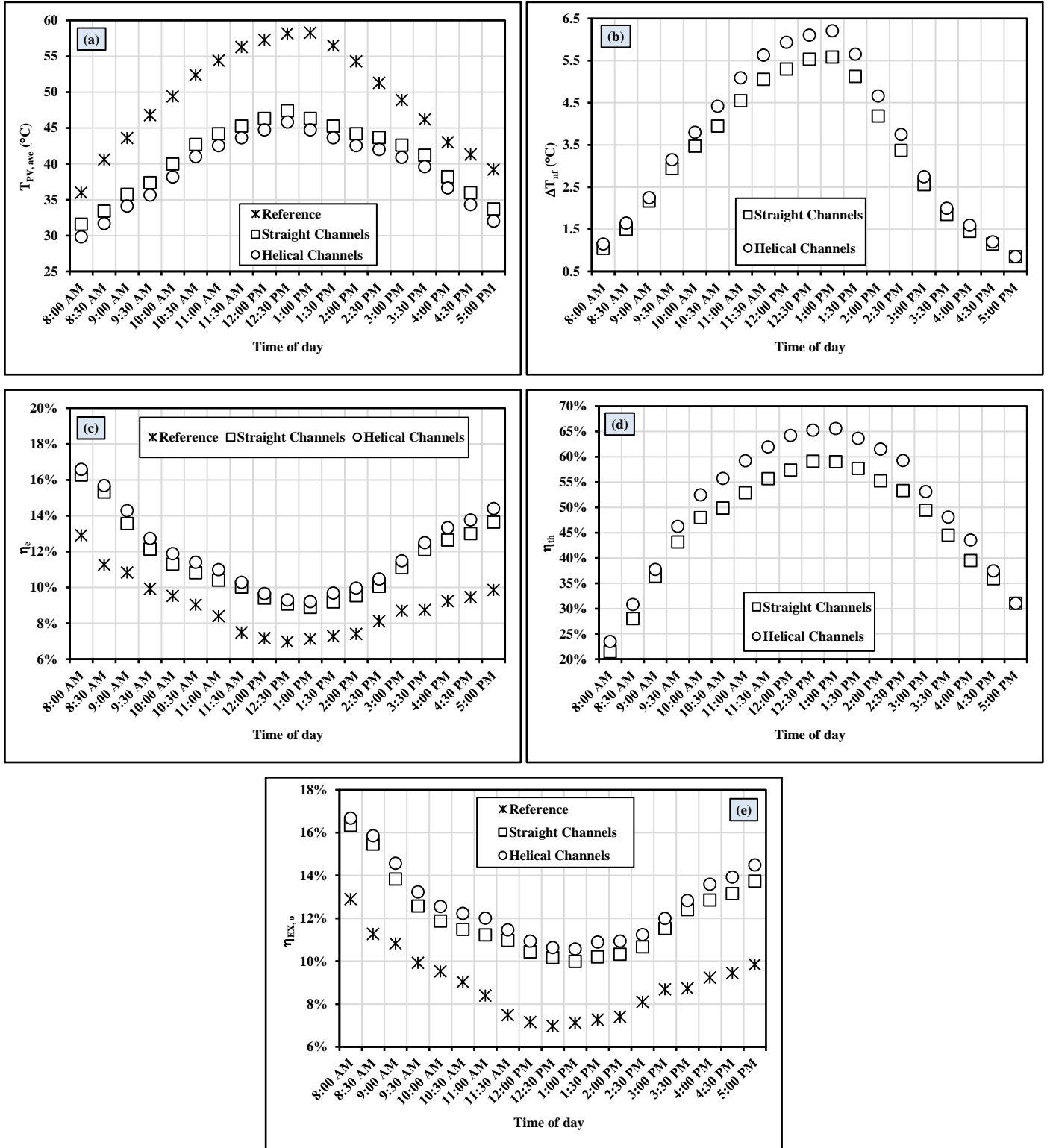


Fig. 6: Effect of channels configuration on PV attributes ($\dot{V}_{nf} = 0.5$ L/min, $\phi = 0.5\%$).

Fig. 6 reveals that the temperature of the panels and the increase in the water or nanofluid temperatures exhibit a similar tendency of the solar irradiation, which initially grow until attaining their extreme values (at around 12:30–1:00 PM), and then they diminish until the sunset. Additionally, applying the cooling whether with straight and helical channels achieves

a noticeable drop in the cells' temperatures. In addition, the helical channels provide a lesser cell temperature and a higher increase in the cooling medium temperature than that of the straight configuration by 1.5°C and 0.4°C, respectively, in average. It is revealed also that the conversion efficiency of the cooled modules is more than that of the standalone PV. At 8 AM, they start high and then a reduction occurs until 1 PM. This is due to the growth in the cell temperature with growing the solar irradiation. As the radiation intensity is going down later, this efficiency is going up due to the diminution in temperature of the cells. It can be noticed also that cooled panel with helical channels has a higher electrical efficiency than that with the straight channel configuration. Compared with the standalone cell, the percentage growth in the conversion efficiency is 42.1% and 50.3%, for using the straight and helical conduits, respectively. Furthermore, it indicated that the thermal efficiency of the system follows the solar intensity changes. It is noticed also that helical configuration provides a higher thermal performance. The PV modules with straight and helical channels provide average thermal efficiencies of 60.6% to 65.7%, respectively. As a result, the exergy efficiency of the cooled panels is always higher than that of the standalone one. It can be observed also that cooled cells with helical conduits have a noticeable growth in the exergy efficiency due to the higher electrical and thermal efficiencies for PVT with this channel configuration. Compared with the standalone cell, the average overall exergy efficiency increases by 42.1% and 50.3% with employing straight and helical conduits, respectively. Despite the higher efficiency of the cooled PV, this needs a pumping power. Therefore, the percentage change in the output power is assessed and compared with the standalone cell.

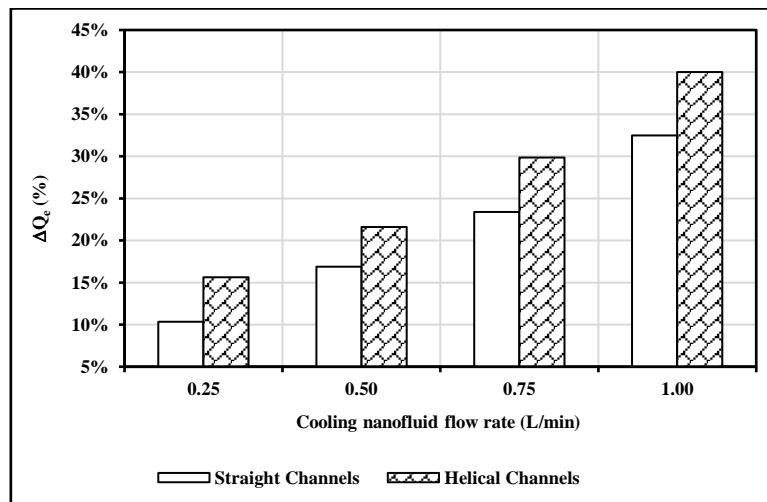


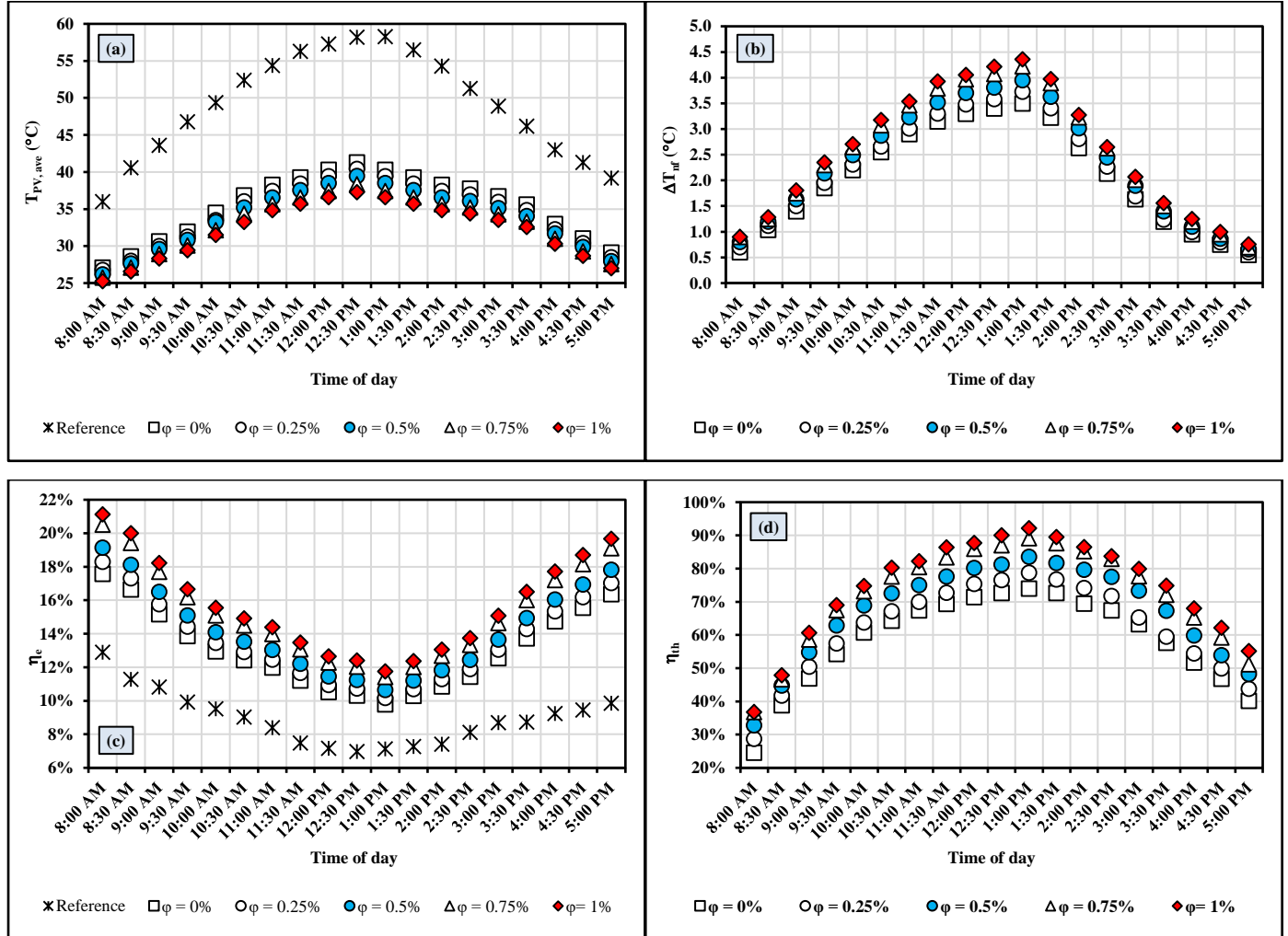
Fig. 7: The average percentage change in the electrical output power at different channels configurations ($\phi = 0.5\%$).

Figure 7 illustrates that employing the helical channels configuration supplies the highest percentage increase in the electrical output power at all operating conditions. The average

increases in the electrical output power are 21.8% and 27.9% when using the straight and helical channels, respectively. This assures that the helical channels configuration is the best configuration as a passive cooling tool for the modules.

4.2 Effect of Nanoparticles Concentration

Figure 8 presents the recorded PV characteristics against different times of the day at different nanoparticles concentrations.



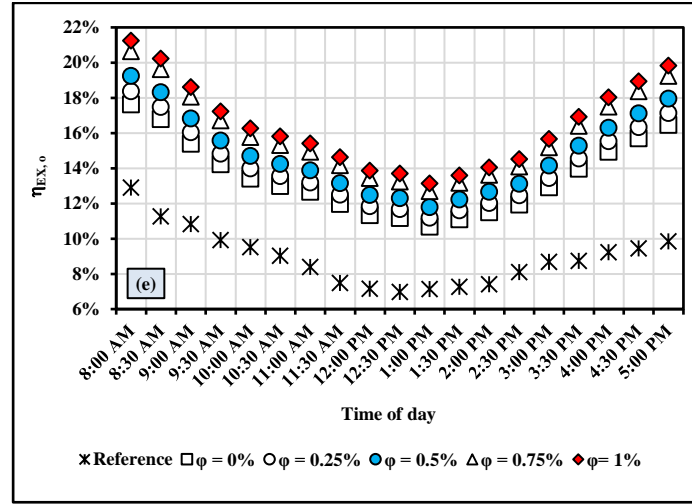


Fig. 8: Effect of nanoparticles concentration on PV characteristics ($V_{nf} = 1$ L/min, Helical Channels).

It is obvious in Fig. 8 that the PV temperature is reduced with loading the nanoparticles. Compared with the standalone cell, the average temperature is decreased from 42.9°C to be 33.6°C and 32.3°C at flow rate of 1 L/min and $\phi = 1\%$ for straight and helical channels, respectively. Furthermore, the PV maximum temperature decreased from 58.3°C for the reference cell to be 39.1°C and 37.3°C at flow rate of 1 L/min and $\phi = 1\%$ for straight and helical channels, respectively. Besides, it is also obvious that increasing the nanoparticles loading augments the increase in the nanofluid temperature. It is observed that at 1 L/min, the maximum ΔT_{nf} increases from 3.2°C and 3.5°C at $\phi = 0\%$ to 4°C and 4.4°C at $\phi = 1\%$ for straight and helical channels, respectively. The reduction in the cell temperature and the increase in the water temperature can be attributed to the augmentation of the rate of heat exchange between the module and the cooling medium with increasing the nanoparticles loading. Adding the nanoparticles enhances the cooling medium thermal conductivity in addition to the nanoparticles Brownian motion. It is revealed also that increasing the nanoparticles volume fraction from 0 to 1% augments the electrical, thermal, and overall exergy efficiencies. Compared with the standalone one, the electrical and exergy efficiencies are increased at flow rate of 1 L/min by 38.2% and 46.1%, respectively, at $\phi = 0\%$, and by 58.4% and 76.4%, respectively, at $\phi = 1\%$, for using the straight and helical channels, respectively. Furthermore, compared with employing pure water ($\phi = 0\%$), increasing the nanoparticles volume concentration to 1% enhances the thermal efficiency at flow rate of 1 L/min by 29.5% and 26.5% with using the straight and helical channels, respectively.

It is clearly shown in Fig. 8 that the conversion efficiency of the cooled panels is higher than that of the uncooled one. Furthermore, increasing the nanoparticles volume fraction enhances

the electrical efficiency of the PV, while it increases the cooling medium viscosity simultaneously, which increases the corresponding pumping power. Fig. 9 establishes the percentage change in the output power of the cooled PVs when compared with that of the standalone one at different nanoparticles concentrations.

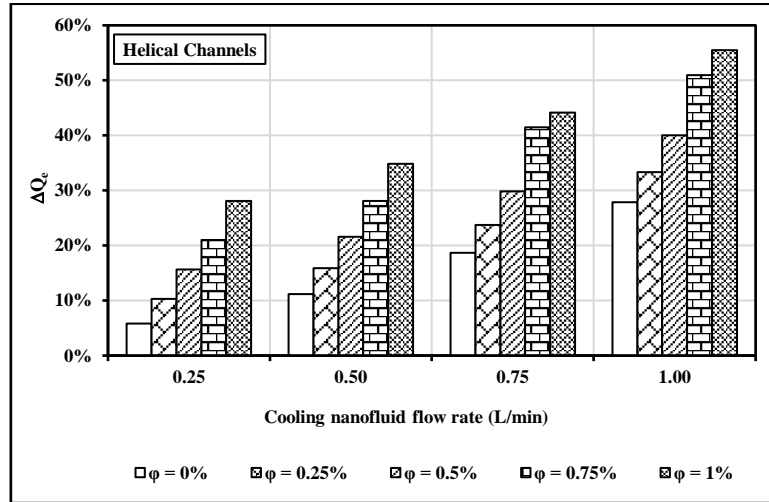


Fig. 9: The average percentage change in the electrical output power at different nanoparticles concentrations.

It is reported that employing the Al_2O_3 nanoparticles enhances the PV electrical power output. Furthermore, this enhancement is augmented with increasing the nanoparticles loading. Compared with the reference cell, circulating the cooling medium at flow rate of 1 L/min and applying the nanofluid of $\phi = 0\%$, the electrical power increases by 1% and 5.8%, while applying the nanofluid of $\phi = 1\%$, the electrical power increases by 47.1% and 55.5% for using the straight and helical channels, respectively.

4.3 Effect of The Cooling Medium Flow Rate

Fig. 10 presents the recorded PV characteristics at different cooling medium flow rates at different times of the day.

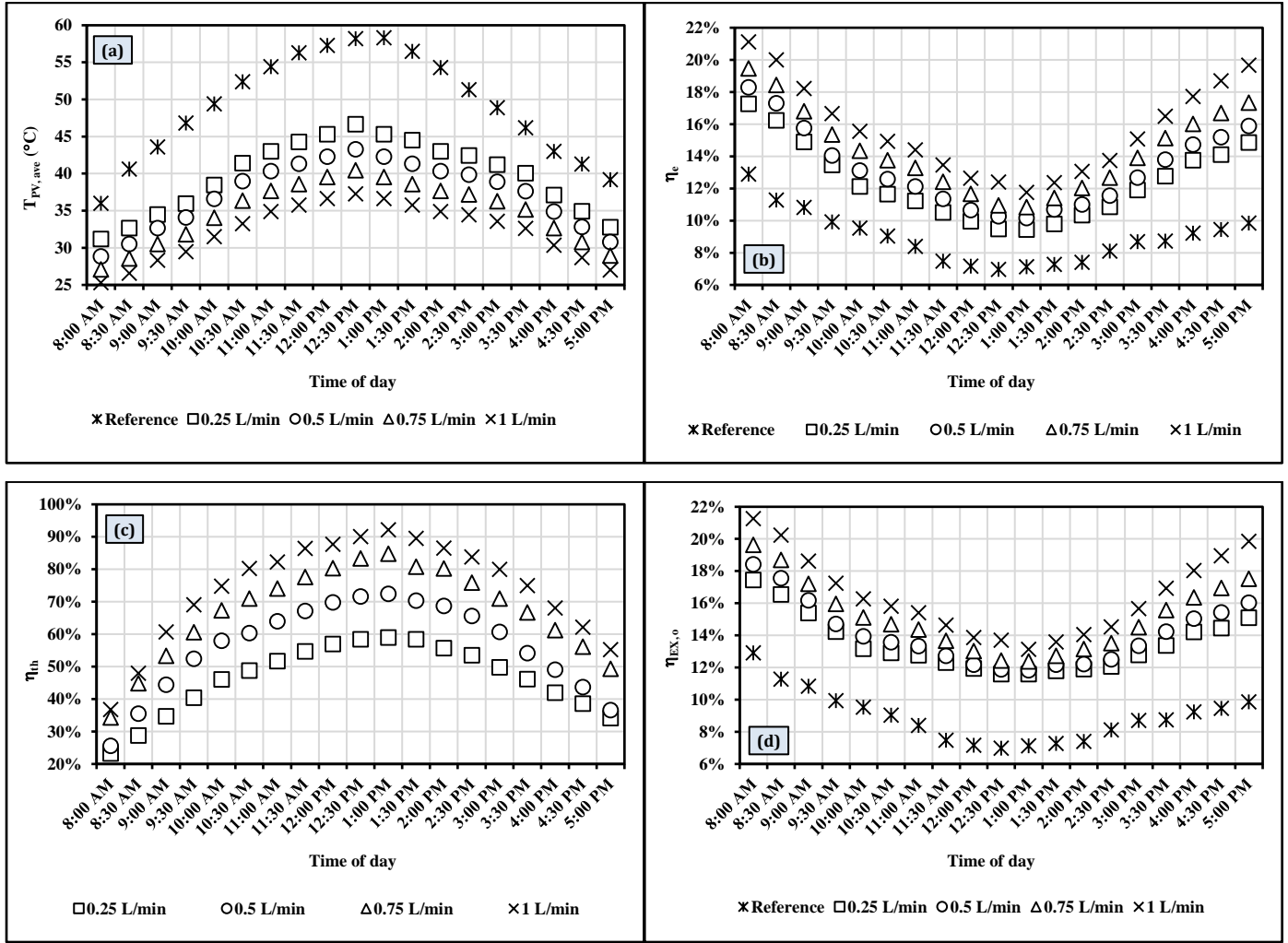


Fig. 10: Effect of cooling medium flow rate on PV characteristics ($\phi = 1\%$, Helical Channels).

It is obvious that increasing the cooling medium from 0.25 to 1 L/min leads to reducing the PV average temperature from 45.2°C to be 36.4°C for the straight channels and from 44.2°C to be 35.2°C for the helical channels. While these temperature reductions are improved with adding the Al_2O_3 nanoparticles. It is recorded at $\phi = 1\%$ that increasing the cooling nanofluid flow rate from 0.25 to 1 L/min leads to reducing the PV average temperature from 41.6°C to be 33.6°C for the straight channels and from 39.7°C to be 32.3°C for the helical channels. This can be attributed to enhancing the fluid mixing and breaking the flow boundary layer with increasing the flow mass flow rate, which enhances the PV cooling. It is revealed also that increasing the water or nanofluid flow rate, from 0 to 1 L/min, augments the electrical, thermal, and overall exergy efficiencies. Compared with the standalone PV, the electrical and exergy efficiencies are increased to 12.3% and 12.7%, respectively, at $\phi = 0\%$, and to 14.8% and 15.7%, respectively, at $\phi = 1\%$, for using the straight channels, while these efficiencies are increased to 13% and 13.5%, respectively, at $\phi = 0\%$, and to 15.7% and 16.4%, respectively, at $\phi = 1\%$,

for using the helical channels. These values correspond to percentage increases of 46.1% and 51.7%, respectively, at $\phi = 0\%$, and to 76.4% and 84.3%, respectively, at $\phi = 1\%$, respectively. Furthermore, compared with flowing the cooling medium with 0.25 L/min, the thermal efficiency is augmented at flow rate of 1 L/min from 31.8% and 34.2% to 51.9% and 58.6% at $\phi = 0\%$ with using the straight and helical channels, respectively. Moreover, the thermal efficiency increases at flow rate of 1 L/min from 42.4% and 46.3% to 67.2% and 74.1% at $\phi = 1\%$ with using the straight and helical channels, respectively. These improvements correspond percentage increases of 63.2% and 71.3%, at $\phi = 0\%$ and of 58.5% and 60%, at $\phi = 1\%$.

It is clearly shown in Fig. 10 that the electrical efficiency of the cooled cells is higher than that of the uncooled one. Furthermore, increasing the cooling medium flow rate enhances the electrical efficiency of the PV, while it increases the corresponding pumping power simultaneously. From Figs. 7 & 9, it is reported that increasing the cooling medium flow rate enhances the PV power output. Compared with the reference cell, increasing the flow rate from 0 to 1 L/min improves the percentage growth in the PV power by 21% and 47.1%, at $\phi = 0\%$ and $\phi = 1\%$, respectively. While this improves the percentage increase in the PV electrical power by 27.8% and 55.5%, at $\phi = 0\%$ and $\phi = 1\%$, respectively, for using the helical channels.

5. Conclusions

The present work considers a hybrid PVT attributes in Cairo conditions. The experiments aim to assess the helpfulness of the usage of $\gamma\text{-Al}_2\text{O}_3$ /water nanofluid in aluminium channels with straight and helical configurations in the PV cooling and usage the thermal energy. The next conclusions can be stated;

- Employing the helical channels configuration supplies the uppermost exergy efficiency besides the highest net electrical power. The average increases in the electrical output power are 21.8% and 27.9% when using the straight and helical channels, respectively.
- The PV temperature is reduced with increasing the nanoparticles loading. The PV maximum temperature decreased from 58.3°C for the reference cell to be 39.1°C and 37.3°C at flow rate of 1 L/min and $\phi = 1\%$ for straight and helical channels, respectively.
- Increasing the nanoparticles volume fraction from 0 to 1% augments the overall exergy efficiency. Compared with the standalone PV, the exergy efficiency is increased at flow rate of 1 L/min by 76.4% at $\phi = 1\%$ for using the helical channels.

- Increasing the nanofluid ($\phi = 1\%$) flow rate from 0 to 1 L/min improves the percentage increase in the PV electrical power by 47.1% and 55.5% for using the straight and helical channels, respectively.

References

- [1] World Energy Council, World Energy Resources 2016, <https://www.worldenergy.org/publications/2016/world-energy-resources-2016/>
- [2] H. Bahaidarah, A. Baloch, P. Gandhidasan, “Uniform Cooling of Photovoltaic Panels: A Review”, Renewable and Sustainable Energy Reviews, vol. 57, pp. 1520–1544, 2016.
- [3] P. Mohanty, T. Muneer, E. Gago, Y. Kotak, “Solar Radiation Fundamentals and PV System Components”, In Solar Photovoltaic System Applications: A Guidebook for Off-Grid Electrification, pp. 7-47, 2016.
- [4] A. Akbarzadeh, T. Wadowski, “Heat Pipe-Based Cooling Systems for Photovoltaic Cells under Concentrated Solar Radiation”, Applied Thermal Engineering, vol. 16(1), pp. 81-87, 1996.
- [5] W.G. Anderson, P.M. Dussinger, D.B. Sarraf, S. Tamanna, “Heat Pipe Cooling of Concentrating Photovoltaic Cells”, Photovoltaic Specialists Conference. PVSC '08. 33rd IEEE, 2008.
- [6] M.J. Huang, P.C. Eames, B. Norton, “Thermal Regulation of Building-Integrated Photovoltaics using Phase Change Materials”, International Journal of Heat and Mass Transfer, vol. 47, pp. 2715–2733, 2004.
- [7] M.J. Huang, P.C. Eames, B. Norton, “Phase Change Materials for Limiting Temperature Rise in Building Integrated Photovoltaics”. Solar Energy, vol. 80, pp. 1121–1130, 2006.
- [8] M.J. Huang, P.C. Eames, B. Norton, “Comparison of a Small-Scale 3D PCM Thermal Control Model with A Validated 2D PCM Thermal Control Model”, Solar Energy Mater. Solar Cells, vol. 90, pp. 1961–1972, 2006.
- [9] J.K. Tonui, Y. Tripanagnostopoulos, “Performance Improvement of PV/T Solar Collectors with Natural Air Flow Operation”, Solar Energy, vol. 82, pp. 1–12, 2008.
- [10] A. Jay, S. Clerc, B. Boillot, A. Bontemps, F. Jay, “Use of Phase Change Material in Order to Maintain the Temperature of Integrated PV Modules at A Reasonable Level”, In: 25th European photovoltaic solar energy conference and exhibition and 5th world conference on photovoltaic energy conversion. Valencia, Spain, 2010.

- [11] E. Cuce, T. Bali, S.A. Sekucoglu, “Effects of Passive Cooling on Performance of Silicon Photovoltaic Cells”, *International Journal of Low-Carbon Technologies*, vol. 0, pp. 1-10, 2011.
- [12] H.G. Teo, P.S. Lee, M.N.A. Hawlader, “An Active Cooling System for Photovoltaic Modules”, *Applied Energy*, vol. 90, pp. 309–315, 2012.
- [13] M. Elmir, R. Mehdaoui, A. Mojtabi, “Numerical Simulation of Cooling a Solar Cell by Forced Convection in the Presence of a Nanofluid”, *Energy Procedia*, vol. 18, pp. 594–603, 2012.
- [14] M. Ozgoren, M.H. Aksoy, C. Bakir, S. Dogan, “Experimental Performance Investigation of Photovoltaic/Thermal (PV-T) System”, *EPJ Web of Conferences*, vol. 45, 01106, 2013.
- [15] İ. Ceylana, A.E. Gürelb, H. Demircanc, B. Aksu, “Cooling of a Photovoltaic Module with Temperature Controlled Solar Collector”, *Energy and Buildings*, vol. 72, pp. 96–101, 2014.
- [16] N. Karami, M. Rahimi, “Heat Transfer Enhancement in a PV Cell Using Boehmite Nanofluid”, *Energy Conversion and Management*, vol. 86, pp. 275–285, 2014.
- [17] A. Aldihani, A. Aldossary, S. Mahmoud, R.K. AL-Dadah, “The Effect of Cooling on the Performance of Photovoltaic Cells under Dusty Environmental Conditions”, *Energy Procedia*, vol. 61, pp. 2383–2386, 2014.
- [18] A. Hasan, S.J. McCormack, M.J. Huang, B. Norton, “Energy and Cost Saving of a Photovoltaic-Phase Change Materials (PV-PCM) System through Temperature Regulation and Performance Enhancement of Photovoltaics”, *Energies*, vol. 7, pp. 1318-1331, 2014.
- [19] S. Nizetic, D. Coko, A. Yadav, F.G. Cabo, “Water Spray Cooling Technique Applied on a Photovoltaic Panel: The Performance Response”. *Energy Conversion and Management*, vol. 108, pp. 287–296, 2016.
- [20] M.R. Salem, R.K. Ali, K.M. Elshazly, “Experimental Investigation of the Performance of a Hybrid Photovoltaic/Thermal Solar System Using Aluminium Cooling Plate with Straight and Helical Channels”, *Solar Energy*, vol. 157, pp. 147-156, 2017.
- [21] L. Tan, A. Date, G. Fernandes, B. Singh, S. Ganguly, “Efficiency Gains of Photovoltaic System Using Latent Heat Thermal Energy Storage”, *Energy Procedia*, vol. 110, pp. 83–88, 2017.

- [22] A. Hasan, J. Sarwar, H. Alnoman, S. Abdelbaqi, “Yearly Energy Performance of a Photovoltaic-Phase Change Material (PV-PCM) System in Hot Climate”, Solar Energy, vol. 146, pp. 417-429, 2017.
- [23] M.R. Salem, M.M. Elsayed, A.A. Abd-Elaziz, K.M. Elshazly, “Performance Enhancement of the Photovoltaic Cells using Al₂O₃/PCM Mixture and/or Water Cooling-Techniques”, Renewable Energy vol. 138, pp. 876–890, 2019.
- [24] Y. Xuan, W. Roetzel, “Conceptions for Heat Transfer Correlation of Nanofluids”, International Journal of Heat and Mass Transfer, vol. 43, pp. 3701–3707, 2000.

Nomenclatures

A	Area, m ²
C _p	Specific heat, J/kg. °C
G	Incident solar intensity (W/m ²)
I	Electrical current, A
\dot{m}	Mass flow rate, kg/s
Q _e	Electric power, W
Q _{in}	Incident solar radiation rate, W
Q _{max}	Maximum output power of PV-module, W
Q _{th}	Thermal heat transfer rate of water or nanofluid, W
T	Temperature, K
t	Time, s
V	Electrical voltage, V
\dot{V}	Volume flow rate, kg/s

Greek Letters

Δ	Percentage change
η	Efficiency
ϕ	Nanoparticles volume concentration

Subscripts

a	Ambient
el	Electrical
i	Inlet
in	Incident
nf	Nanofluid
np	Nanoparticle

o	Outlet
oc	Open circuit
S	Solar
sc	Short circuit
th	Thermal
w	Water

Acronyms and Abbreviations

PCM	Phase change material
PV	Photovoltaic
PVT	Photovoltaic thermal